A Leaky Human Colon Model Reveals Uncoupled Apical/Basal Cytotoxicity in Early *Clostridioides difficile* Toxin Exposure

Meryem T. Ok[1,5], Jintong Liu[2,5], R. Jarrett Bliton[1], Caroline M. Hinesley[2], Ekaterina Ellyce T. San Pedro[2], Keith A. Breau[3], Ismael Gomez-Martinez[3], Joseph Burclaff[1,2], Scott T. Magness[1,2,3,4*]

[1] Joint Department of Biomedical Engineering, University of North Carolina at Chapel Hill and North Carolina State University, Chapel Hill, North Carolina
[2] Center for Gastrointestinal Biology and Disease, University of North Carolina at Chapel Hill and North Carolina State University, Chapel Hill, North Carolina
[3] Department of Cell Biology and Physiology, University of North Carolina at Chapel Hill, Chapel Hill, North Carolina
[4] Department of Medicine, University of North Carolina at Chapel Hill, Chapel Hill, North Carolina
[5] These authors contributed equally
* Correspondence: magness@med.unc.edu

Grant Support: Supported by National Institutes of Health grants R01DK115806 (S.T.M.), R01DK109559 (S.T.M.), P30DK034987 (S.T.M.), National Science Foundation grant CBET-1934284 (S.T.M.), and the Katherine E. Bullard Charitable Trust for Gastrointestinal Stem Cell and Regenerative Research (S.T.M.), F32DK124929 (J.B.), T32GM133364 (K.A.B).

Abbreviations used in this paper: ACC (absorptive colonocyte), AE (absorptive enterocyte), CDI (*Clostridioides difficile* infection), CDT (*Clostridioides difficile* transferase), DC (descending colon), DCF (diclofenac), DM (differentiation media), EM (expansion media), FAE (follicle-associated epithelium), hCE (human colonic epithelium), hSIE (human small intestinal epithelium), IBD (inflammatory bowel disease), ISC (intestinal stem cell), NSAID (nonsteroidal anti-inflammatory drug), PC (principal component), scRNAseq (single-cell RNA-sequencing), TA (transit-amplifying), TcdA (Toxin A), TcdB (Toxin B), TEER (transepithelial electrical resistance), 3D (3-dimensional)

Disclosures: STM has a financial interest in Altis Biosystems Inc., which licenses the technology used in this study. The remaining authors disclose no conflicts.

Author contributions:

- **Meryem T. Ok**: Formal Analysis (Lead); Investigation (Lead); Methodology (Lead); Visualization (Lead); Writing – original draft (Lead), Writing – review & editing (Lead)
- **Jintong Liu**: Formal Analysis (Lead); Investigation (Lead); Methodology (Lead); Visualization (Supporting); Writing – original draft (Lead); Writing – review & editing (Supporting)
- **R. Jarrett Bliton**: Data curation (Lead); Formal Analysis (Supporting); Visualization (Supporting); Writing – review & editing (Supporting)
- **Caroline M. Hinesley**: Formal Analysis (Supporting); Investigation (Supporting)
- **Ekaterina Ellyce T. San Pedro**: Investigation (Supporting); Methodology (Supporting)
- **Keith A. Breau**: Data curation (Lead); Formal Analysis (Supporting); Visualization (Supporting); Writing – review & editing (Supporting)

- **Ismael Gomez-Martinez**: Methodology (Supporting); Visualization (Supporting); Writing – review & editing (Supporting)
- **Joseph Burclaff**: Formal Analysis (Supporting); Visualization (Supporting); Writing – review & editing (Supporting)
- **Scott T. Magness**: Conceptualization (Lead); Funding acquisition (Lead), Project Administration (Lead); Supervision (Lead); Writing – review & editing (Equal)

Synopsis: Novel human colonocyte cultures, benchmarked by transcriptomics for physiological relevance, detect the earliest cytopathic impacts of *Clostridioides difficile* toxins. Basal TcdA/B exposure generally caused more rapid onset and cytotoxicity than apical exposure. Diclofenac-induced leaky epithelium enhanced apical exposure toxicity.

ABSTRACT

Background & Aims: *Clostridioides difficile* (*C. difficile*) toxins A (TcdA) and B (TcdB) cause antibiotic-associated colitis and increase morbidity and mortality. Accurate in vitro models are necessary to detect early toxicity kinetics, investigate disease etiology, and develop pre-clinical models for new therapies. Properties of cancer cell lines and 3D organoids inherently limit these efforts. Here, we develop adult stem cell-derived monolayers of differentiated human colonic epithelium (hCE) with barrier function, investigate the impact of toxin application to apical/basal aspects of monolayers, and evaluate whether a leaky epithelial barrier enhances toxicity.

Methods: Single-cell RNA-sequencing (scRNAseq) mapped *C. difficile*-relevant genes to cell lineages across the human gut. Transcriptomics informed timing of stem cell differentiation to achieve in vitro colonocyte maturation like that observed in vivo. Transepithelial electrical resistance (TEER) and fluorescent dextran permeability assays measured cytotoxicity as barrier loss post-toxin exposure. Leaky epithelial barriers were induced with diclofenac.

Results: scRNAseq demonstrated broad and variable toxin receptor expression across the human gut lineages. Absorptive colonocytes displayed generally enhanced toxin receptor, Rho GTPase, and cell junction expression. 21-day differentiated Caco-2 cells remained immature whereas hCE monolayers were similar to mature colonocytes. hCE monolayers exhibited high barrier function after 1-day differentiation. Basal TcdA/B application to monolayers caused more toxicity and apoptosis than apical exposure. Diclofenac induced leaky hCE monolayers and enhanced toxicity of apical TcdB exposure.

Conclusions: Apical/basal toxicities are uncoupled with more rapid onset and increased magnitude of basal toxicity. Leaky paracellular junctions enhance toxicity of apical TcdB exposure. hCE monolayers represent a physiologically relevant and sensitive culture system to evaluate the impact of microbial toxins on gut epithelium.

Key words: Intestinal Stem Cells; Absorptive Colonocyte Monolayers; Toxicity; Permeability

INTRODUCTION

Clostridioides difficile is a toxin-producing bacterium that causes *C. difficile* infection (CDI), with symptoms ranging from mild diarrhea to severe colitis and associated with life-threatening illnesses such as toxic megacolon and bowel perforation.[1] CDI has a tremendous economic burden, costing an estimated $6.3 billion in annual healthcare expenses in the U.S. alone.[2] Patients with greater CDI risk include those who are immunocompromised, receiving broad-spectrum antibiotics, or battling a leaky gut, often due to underlying chronic illness such as inflammatory bowel disease (IBD).[2, 3] While fidaxomicin and vancomycin remain first-line antibiotics for patients with CDI, the high treatment costs,[4] emergence of antibiotic-resistant strains,[5] and increase in recurrence rates[6] especially for hypervirulent strains (≥ 23%)[6, 7] are growing problems.

C. difficile damages the colonic epithelium by secreting Toxin A (TcdA), Toxin B (TcdB), and binary toxin *C. difficile* transferase (CDT). CDT is produced by approximately 20% of *C. difficile* strains, but it receives less clinical attention given that CDT-producing strains lacking TcdA and TcdB are nontoxigenic in vitro.[8, 9] TcdA and TcdB (TcdA/B) are homologous glucosyltransferases that bind to various host cell receptors, enter cells via endocytosis, and inactivate Rho-family GTPases by monoglucosylation.[10] This ultimately results in cytoskeletal disassembly, tight junction collapse, cytopathic cell rounding, and eventual apoptosis.[11-15] While the TcdA/B receptor distribution likely impacts the onset of cytopathic events, this distribution has not been thoroughly mapped across the proximal-distal axis of the human gut or across epithelial cell lineages. A comprehensive map of *C. difficile* toxin receptors across all undifferentiated and differentiated lineages would address a major gap in knowledge and serve as a foundation to better understand mechanisms of toxin interactions with the epithelium, disease onset, progression, and resolution.

Alternatives to antibiotic therapies are becoming an attractive approach to treat CDI; however, physiologically relevant preclinical models of the human colon to test new therapies are lacking. Historically, *C. difficile* toxicity models relied on non-intestinal cell types (e.g., Vero, HeLa) or colon cancer cell lines (e.g., T84, HT-29, Caco-2).[16-19] However, colon cancer cells do not express physiological transporters/carriers found in healthy human colonic epithelium (hCE), and they phenotypically resemble small intestinal enterocytes.[20, 21] While TcdB is more cytotoxic than TcdA in T84 cells and non-intestinal epithelium,[22, 23] TcdA is more potent than TcdB in 3D human intestinal organoids (HIOs) and jejunal enteroid-derived monolayers.[24, 25] Although a significant improvement in physiological accuracy, 3D organoids—in which the apical cell surface faces inward inside an enclosed epithelium—do not allow easy simultaneous access to apical/basal cell surfaces to apply toxins or assess barrier function using transepithelial electrical resistance (TEER) or permeability assays. Moreover, HIOs are induced to differentiate from pluripotent stem cells in vitro and the resulting organoids are more similar to fetal small intestine[26] than colon, which is the predominant site of CDI,[27] giving these findings limited generalizability to the sensitivity of adult differentiated hCE to TcdA/B. Thus, more physiologically accurate culture systems are essential to mimic in vivo colonic epithelium and investigate the impact of TcdA/B on hCE.

Currently, there are no established quantitative culture systems that simultaneously evaluate the apical versus basal impact of TcdA/B on hCE. *C. difficile* toxins are secreted in the lumen and thought to interact first with the apical aspect of the intestinal or colonic epithelial barrier.[28] However, receptor studies in colon cancer cell lines[28, 29] and in non-human, non-

intestinal epithelial cells[30] reveal that some TcdA receptors locate to the basal side of the cell, making them inaccessible to TcdA when there is an intact physiological epithelial barrier. This raises the possibility that a healthy epithelial barrier may be more refractory to apical TcdA cytotoxicity than previously believed, but this has yet to be tested in hCE. Likewise, while some TcdB receptors localize to the basal aspect of the epithelium,[31-33] their full apical/basal distribution remains unclear,[34, 35] though functional studies in HIOs show distinct apical and basal differences in barrier disruption.[24] Thus, we designed a model to quantify the magnitude and time-course of apical/basal toxicity, which could inform whether early clinical interventions should target apical versus basal hCE.

Here, we establish a physiologically relevant in vitro model of *C. difficile* TcdA/B toxicity using primary adult intestinal stem cell (ISC)-derived hCE monolayers. Building upon our previous methods of culturing primary ISCs from healthy human donor organs and differentiating these ISCs into a functional epithelial layer,[36-38] we develop a highly sensitive assay system for evaluating early-stage intestinal barrier injury and late-stage cytotoxic events associated with TcdA/B. Our tissue engineering approach focuses on producing an epithelium that closely mimics in vivo colonic tissue, which we use to assess *C. difficile*-relevant transcriptional and phenotypic differences between hCE, human small intestinal epithelium (hSIE), and Caco-2 cells. Using this system, we test the temporal dynamics of apical and basal TcdA/B toxicity, measure the effect of a leaky epithelium on toxin activity, and present biological insights into the impact of apical and basal cytotoxicity of TcdA/B.

RESULTS

A Single-Cell Survey of Human Gut Epithelium Reveals Organ and Lineage Variability of *C. difficile* Toxin-Relevant Genes

Expression of *C. difficile*-relevant gene sets have not been characterized across the epithelial lineages of the small intestine and colon. To address this, we interrogated single-cell transcriptomic data across all lineages in small intestine and colon from three healthy human adult donors **(Fig. 1A)**[39] and evaluated the magnitude of toxin receptor expression **(Fig. 1B)**.[28, 29, 31, 34, 40, 41] In general, the ISC, transit-amplifying (TA), and absorptive lineages in the small intestine and colon exhibited more toxin receptor expression and with higher magnitudes compared to the secretory lineages. Notably, follicle-associated epithelium (FAE) uniquely expressed high levels of the TcdB receptor *FZD7* **(Fig. 1B)**. Lineage-specific *C. difficile* toxicities have not been evaluated; thus, these findings provide a foundation to investigate such questions.

Next, we sought to evaluate the *C. difficile*-relevant genes in the two key cell types involved in the initiation and resolution of *C. difficile* infections. The absorptive lineages are the predominant cell types in the small intestine and colon and experience first-line exposure to *C. difficile*, and the ISCs are responsible for regenerating the epithelium after damage. We surveyed curated gene sets for toxin receptor, Rho GTPase, and tight junction expression in ISCs and mature absorptive cells in six regions across the proximal-distal axis of the small intestine (Duodenum, Jejunum, Ileum) and colon (Ascending, Transverse, Descending) **(Fig. 2A)**. For the toxin receptor genes, sucrase-isomaltase is a small intestine-specific brush border enzyme;[42] thus, it is not expected to be meaningfully expressed in the colon, as demonstrated by the data **(Fig. 2A)**. When comparing the remaining receptors between small intestinal and colonic ISCs, there was no difference in *HSP90B1* and *LSR*, *FZD5* was significantly higher in colonic ISCs, and *LRP1* and *NECTIN3* were higher in small intestinal ISCs **(Fig. 2B)**. In mature absorptive cells of the small intestine and colon, all receptors except for *LRP1* and small intestinal-specific *SI* were significantly higher in colon **(Fig. 2B)**. For classic Rho-family GTPases (*CDC42, RAC1,* and *RHOA*),[43-45] which are terminal targets of *C. difficile* toxins, no specific gene demonstrated statistically significant differences between small intestinal and colonic ISCs **(Fig. 2C, D)**. However, in mature absorptive lineages, *RAC1* was modestly but significantly higher in small intestine, and *CDC42* and *RHOA* were higher in the colon **(Fig. 2C, D).**

We analyzed tight junction proteins, which are known to be disrupted as a terminal effect of toxin-induced Rho GTPase glucosylation.[14] A subset of 34 genes were selected from a published curated gene set based on classification of 'tight junction' or 'tight junction-associated' genes.[46] Fifteen genes with the highest mean expression in mature small intestinal and colonic absorptive lineages were grouped by transmembrane versus intracellular proteins and their expression was characterized across regions and lineages of the small intestine and colon **(Fig. 2E)**. Claudin (*CLDN*) genes *CLDN3*, *CLDN4*, and *CLDN7*, which aid in forming selective barriers to macromolecules (such as *C. difficile* toxins) and ions,[47] are highly expressed across all ISCs and mature absorptive cells, with notably higher expression in mature absorptive lineages of the colon **(Fig. 2F)**. *CLDN15* showed unique and high expression in the ISCs and mature absorptive lineages of the small intestine. ISCs and mature absorptive lineages across all small intestinal and colonic regions demonstrated broad expression of the remaining tight junction genes, which were generally expressed at lower magnitude than the claudins **(Fig. 2F).** These findings highlight

variability in small intestinal and colonic regions and lineages that could lead to functional differences in intestinal epithelial barrier function and likely influence CDI onset and progression.

Transcriptomics Show hCE Monolayers Mature Over Time to Mimic In Vivo Mature Absorptive Colonocytes

With the single-cell transcriptomic data serving as the in vivo benchmark for physiological relevance, we sought to determine whether colonic ISCs could be differentiated in vitro to closely mimic the absorptive colonocytes in vivo. We also compared the transcriptomics of differentiated hCE monolayers to differentiated Caco-2 monolayers in an effort to establish which model more closely aligned to in vivo transcriptomic lineage states. To differentiate hCE monolayers, primary crypt-derived ISCs from the descending colon (DC) were first expanded on collagen-coated hydrogels as previously described.[38] DC tissue was chosen given that CDI primarily manifests as colitis in the distal colon.[27] Once confluent, these cells were then plated onto Matrigel-coated Transwell™ inserts in expansion media (EM) containing ISC growth factors (Wnt3a, R-spondin 3, and Noggin) for 4 days during which they continued to proliferate to form a confluent monolayer. To differentiate the colonic ISCs, differentiation media (DM) was applied to ISCs for an additional 4 days **(Fig. 3A)**. RNA was isolated from hCE monolayers at various timepoints (EM Day 1, EM Day 4 = DM Day 0, DM Day 2, and DM Day 4), and transcriptomics was used to verify differentiation and characterize cell maturation.

Principal component analysis showed subtle transcriptomic changes while in EM (EM D1, DM D0) but substantial changes along principal component (PC) 1 and PC2 after 2 days of differentiation (DM D2), indicating large expression changes between Day 0 and Day 2 of colonic ISC differentiation **(Fig. 3B)**. There were fewer transcriptomic changes between Day 2 and Day 4 of differentiation, indicating relatively stable transcriptomes during this time window. We compared hCE transcriptomics to 21-day differentiated Caco-2 to determine if Caco-2 transcriptomics tracked with the differentiated hCEs. Caco-2 cells were markedly separated from colonic ISCs and all stages of hCE differentiation in PC1, highlighting that differentiated Caco-2 monolayers are significantly different than the primary tissue-derived hCE monolayers **(Fig. 3B)**.

We further characterized the differentiation of hCE monolayers at a more granular level to determine if time of differentiation could "mature" the monolayers to a transcriptomic state that resembles mature absorptive colonocytes in vivo. We curated two gene sets from the in vivo single-cell transcriptomic data as the standard for comparison, one from the colonic ISCs and one from the mature absorptive colonocytes (i.e. late ACCs).[39] The hypothesis was that replacement of EM with DM would shift the transcriptomic state of the monolayers away from the ISC signature and closer to the mature absorptive colonocyte signature. The data show that hCE monolayers at EM Day 1 are more closely aligned with the in vivo colonic ISC signature, but these similarities decrease over four days of differentiation where the magnitude of most colonic ISC genes is reduced **(Fig. 3C)**. By contrast, 21-day differentiated Caco-2 cells still exhibit higher expression of many colonic ISC genes, notably *LGR5* and *ASCL2* **(Fig. 3C)**.

Conversely, when gene signatures of hCE and Caco-2 monolayers are compared to the in vivo late ACC signature, hCE cells show increased magnitude of gene expression at DM Day 2 which stabilized through DM Day 4 **(Fig. 3D)**. In most instances, the 21-day differentiated Caco-2 genes more closely aligned with the expression patterns of EM Day 1 and DM Day 0, which is reflective of a persistent undifferentiated state and further highlights the less mature state of

differentiated Caco-2 **(Fig. 3D)**. To characterize the extent of the undifferentiated state between differentiated hCE and Caco-2 monolayers, curated gene sets associated with S- and G2/M-phase cell cycle stages were analyzed.[48] We hypothesized that differentiated hCE monolayers would express relatively lower levels of S- and G2/M-phase genes while Caco-2 monolayers would show upregulated expression of these genes. The data show that 21-day differentiated Caco-2 monolayers express higher levels of nearly all genes associated with cell cycling, notably the cell proliferation markers *MKI67* and *PCNA* **(Fig. 3E)**. Finally, gene set enrichment analyses were performed using the full gene signature of in vivo colon ISCs (108 genes) and in vivo late ACCs (215 genes).[39] Consistent with our earlier observations, Caco-2 monolayers are significantly enriched for stem-like genes compared to hCE monolayers **(Fig. 3F)**, whereas hCE monolayers are significantly enriched for late ACC genes compared to Caco-2 monolayers **(Fig. 3G).** These findings emphasize that hCE monolayers are more terminally differentiated and more aligned with the in vivo late ACC gene signature, which likely translates into better functional equivalence compared to Caco-2 cells.

Differentiated hCE Monolayers Exhibit Stronger TEER Barrier Properties Than Caco-2 or hSIE Monolayers

Our findings point to substantial gene expression differences in lineage states between differentiated hCE and Caco-2 monolayers. Human small intestinal organoids and monolayers have been used to model TcdA/B toxicities; thus, we also compared barrier functions of hCE and hSIE monolayers. In prior work, we established a method for culturing healthy human jejunal monolayers and tracking cell maturation using transepithelial electrical resistance (TEER),[36] a non-invasive quantitative technique that is widely accepted to measure epithelial integrity.[49] Here, we applied similar principles to differentiated hCE (DC), hSIE, and Caco-2 monolayers and characterized the variation in barrier properties as measured by TEER between multiple donors **(Fig. 4A).**

Daily TEER measurements were performed during monolayer expansion and differentiation **(Fig. 4B)**. In hCE monolayers from three healthy human donors, TEER was measured for 4 days in EM followed by 4 days in DM **(Fig. 4C)**. After just one day of DM exposure, hCE TEER reached an average value of 1000-2000 $\Omega \times cm^2$, consistent with a tight epithelial barrier.[49] While the individual TEER profiles varied by donor, the steep increase in hCE TEER after switching to DM was consistent across all three donors. It is noteworthy that both Caco-2 and hSIE monolayers did not reach high resistance like hCE cultures, with values staying below 500 $\Omega \times cm^2$ **(Fig. 4D, E).** This finding is consistent with previous jejunal TEER studies even after 12 days of differentiation,[36] supporting the notion that hCE monolayers have a different barrier strength profile than hSIE or Caco-2 monolayers, which exhibit lower barrier strength profiles. Thus, differentiated Caco-2 cells, which have a baseline TEER that is much lower than that of differentiated hCE and is more consistent with ISCs and hSIE, may not accurately report *C. difficile* toxin sensitivities in the colon.

Colonic Monolayers Exhibit a Dose-Dependent Early Cytotoxicity to TcdA, but Not TcdB, After Apical Exposure

By Days 2-4 of differentiation, hCE show transcriptional signs of maturation **(Fig. 3B, D)** and TEER is sufficiently elevated, indicating a tight barrier **(Fig. 4C)**. A drop in TEER at later

timepoints is inherent to these differentiated primary culture systems since these cells undergo a natural ~5-day lifespan after leaving the stem/progenitor cell state. Interestingly, this may be an intrinsically programmed lifespan as mouse and human epithelial cells in vivo exhibit a similar lifespan.[50] Given these features of the culture system, toxin experiments were initiated on Day 3 of differentiation at time t = 0 **(Fig. 5A)** as this was between 2 timepoints that closely mimic the in vivo maturation state, exhibits a relatively high barrier function as measured by TEER, and provides a sufficient window to perform toxicity assays prior to the cells' terminal lifespan.

To evaluate the sensitivity of the system to detect cytotoxic effects by TEER, three doses of TcdA and TcdB were applied apically to mature hCE monolayers. A dose of 30 pM was used as 1X as this is a physiological concentration identified in patients with active CDI.[51] TcdA or TcdB at doses of 30 pM (1X), 150 pM (5X), and 300 pM (10X) were applied to differentiated hCE, and TEER changes were monitored during the first 12 hours and after 24 hours based on prior evidence of cytotoxicity within that timeframe **(Fig. 5B)**.[25, 52] hCE monolayers apically exposed to TcdB at any dose did not show a significant drop in TEER over 24 hours of exposure. Unlike TcdB, TcdA demonstrated a dose-dependent toxicity whereby 5X and 10X increasingly hastened the onset of barrier loss as measured by TEER **(Fig. 5B)**. These findings indicate that the hCE culture system is sufficiently sensitive to detect the impact of clinically relevant concentrations of TcdA and shows that TcdA apical exposure is more toxic than TcdB apical exposure at a molar-to-molar ratio.

Basal Exposure to *C. difficile* Toxins A/B Produces More Rapid and Severe Cytotoxicity Than Apical Toxin Exposure

The lack of overt TcdB cytotoxicity when applied to the apical aspect of hCE monolayers was surprising given that TcdB is associated with severe toxicity in other systems.[22, 23, 53] The observation that differentiated hCE monolayers were refractory to apical TcdB exposure prompted the question as to whether hCE and hSIE monolayers possess inherently different apical and basal toxin sensitivities. Etiologically, this is an important distinction to evaluate since our data imply that a healthy hCE monolayer may be highly resistant to apical *C. difficile* toxins. If TcdA/B have more potent effects when in contact with the basal aspect of cells, then CDI may primarily promote clinical sequelae when the epithelial barrier is compromised due to conditions that cause a leaky gut epithelium, at which point TcdA/B can access the basal aspect of the cell and cause rapid onset of toxicity. To evaluate differential sensitivities of apical and basal *C. difficile* toxin at a molar-to-molar ratio, 1X (30 pM) toxin was applied to either the apical or basal reservoirs of Transwells with differentiated hCE or hSIE monolayers from three separate human donors **(Fig. 5C, D)**.

TcdB applied to the apical aspect of differentiated hCE monolayers from three different donors demonstrated either no cytotoxicity or limited and delayed toxicity at 12 hours post-TcdB exposure **(Fig. 5C)**. By contrast, there was rapid and substantial cytotoxicity as early as 2 hours (on average, ~4.7 hours) when TcdB was applied to the basal aspect of the monolayers across all donors. Similarly, there was a trend of significantly delayed toxicity for TcdA when applied to the apical aspect of the monolayers compared to when TcdA was applied to the basal aspect of cells. For 2 donors, the monolayers demonstrated limited apical TcdA cytotoxicity at 12 hours, whereas basal exposure to TcdA resulted in rapid onset of cytotoxicity as early as 2 hours (on average, 4 hours) post-exposure across all three donors **(Fig. 5C)**. Interestingly, Donor 2 monolayers were more sensitive to apical application of both TcdA/B, and Donor 3 monolayers demonstrated

delayed onset of cytotoxicity for both TcdA/B compared to the other two donor monolayers. Overall, TcdA/B demonstrated more cytotoxicity when exposed to the basal aspect of cells. Consistent with this, hCE monolayers were refractory to apoptosis at 24 hours after apical TcdA or TcdB exposure, while basal toxin exposure caused obvious signs of apoptosis **(Fig. 5E)**. Differential toxin sensitivities observed between donors is interesting and may reflect genetic backgrounds that render the differentiated hCE monolayers more or less responsive to the mechanisms of toxicity, which could be useful for determining patient-specific responses.

Single-cell RNAseq data of the *C. difficile* receptor gene expression profiles demonstrated that 2 out of the 3 known TcdA receptor genes (*SI* and *LRP1*) have significantly higher gene expression in mature absorptive lineages of the small intestine versus colon **(Fig. 2B)**. Thus, we hypothesized that differentiated hSIE monolayers would be more sensitive than differentiated hCE monolayers to TcdA. When TcdA was applied to the apical aspect of monolayers, substantial cytotoxicity was observed in hSIE monolayers as early as 2 hours (on average, 4 hours) **(Fig. 5D)**. By comparison, differentiated hCE demonstrated limited apical TcdA cytotoxicity in 2 donors with a late onset of 12-24 hours (on average, 12 hours across all donors) **(Fig. 5C)**. These findings show that differentiated hSIE is more sensitive to apical exposure to TcdA compared to differentiated hCE. Of note, TcdA/B cytotoxicity in Caco-2 monolayers is more consistent with trends observed in the hSIE monolayers compared to the hCE monolayers, with rapid sensitivity to apical TcdA within 2-4 hours and a relatively slower response to basal TcdB **(Fig. 5F)**. This highlights that, despite being derived from colon epithelial cancer, Caco-2 cells respond to toxins more like hSIE than hCE monolayers.

A Leaky hCE Induced by NSAIDs Reduces Apical Barrier Protection From TcdB

Our results so far suggest limited sensitivity to TcdB on the apical/luminal surface of the human colon, but enhanced TcdB toxicity when applied to the basal surface. We hypothesized that toxin translocation from the apical to the basal side may be initiated or enhanced by a "leaky gut", a term used to describe a broad range of underlying genetic, disease, or injury states that create increased intestinal paracellular permeability.[54] Nonsteroidal anti-inflammatory drugs (NSAIDs) in general are associated with colitis,[55] and diclofenac (DCF) in particular has demonstrated a significantly increased risk of *C. difficile*-associated diarrhea.[56, 57] Diclofenac, a commonly prescribed NSAID, has been previously shown to induce a leaky gut in primary hSIE.[58] Clinically-relevant dosing of 1 mM was determined based on translating a typical therapeutic dose of 50 mg oral diclofenac into local concentrations of diclofenac between 300-1600 µM within the intestinal lumen.[59-61]

While TEER is an effective method to monitor ion flux across a damaged epithelial monolayer, it may not accurately report flux of toxin-sized molecules. To test whether a leaky gut induced by diclofenac initiates apical-to-basal translocation of toxin-sized molecules, a permeability assay was designed using hCE monolayers to monitor the translocation of conjugated dextrans from the apical to basal reservoir after toxin exposure **(Fig. 6)**. Large molecular weight dextrans should remain in the apical reservoir of the Transwells if there is a healthy epithelial barrier. FITC-Dextran (250 kDa) was chosen because it is similar to the molecular weight of TcdB (~270 kDa), which would provide insight into the time course in which a TcdB-sized particle would be able to pass paracellularly when the epithelial barrier is damaged. In the first 12 hours, apical diclofenac exposure alone induced modest leakiness which was

compounded by the apical addition of TcdB, as measured by FITC-Dextran permeability **(Fig. 6)**. Of all the TcdB experimental conditions, increased permeability was only observed in the diclofenac/TcdB condition at 12 hours, consistent with the idea that epithelial barrier damage was allowing TcdB to interact with the basal aspect of the monolayer. At 24 hours, apical diclofenac/TcdB continued to show significantly increased permeability of FITC-Dextran, trending toward permeability levels that are only induced by direct application of TcdB to the basal side of the hCE monolayer **(Fig. 6)**. Taken together, these findings further reveal that a leaky colonic epithelial barrier can enhance the cytotoxic effects of apical TcdB exposure, likely through a mechanism whereby TcdB gains access to the basal aspect of the epithelial monolayer.

DISCUSSION

In this work, we describe uncoupled apical and basal toxicity of *C. difficile* TcdA/B on hCE in multiple healthy human donors. We demonstrate that toxin sensitivities differ between hCE and hSIE, which could be related to different magnitudes of toxin receptor distribution across anatomical regions of the gut as revealed by our transcriptomic data. This interpretation is supported by findings that some toxin receptors are preferentially located on the apical versus basal surface of small intestinal or colonic epithelium.[28-33, 40] The importance of identifying uncoupled apical/basal magnitude and time course of TcdA/B cytotoxicities may help inform the approach to develop more effective therapeutic modalities. As basal toxin exposure has more substantial cytotoxic effects, the use of luminal therapeutics such as probiotics or toxin-neutralizing drugs could be used as prophylaxis to prevent toxins from reaching the basal surface where they have more potent effects. This also has important clinical implications for patients with underlying intestinal epithelial barrier dysfunction, suggesting that they may have greater sensitivity to *C. difficile* toxins due to basal receptor interactions.

While 3D organoids and 2D monolayers are becoming more widely used to study host-microbe interactions, here we specifically tailor and characterize a first-in-kind 2D monolayer system in vitro that closely mimics the transcriptomic state of late ACCs found in vivo. We then focus the assay development in the system to detect the first signs of barrier loss caused by *C. difficile* toxins. Although preclinical intestinal models traditionally focus on genetically homogenous Caco-2 cells and other cell lines,[16-19, 62-65] our transcriptomic data and barrier strength readouts show that Caco-2 cells remain in a relatively undifferentiated state and have a more similar barrier function profile to hSIE monolayers. This suggests that the hCE monolayers developed in our system are likely a more accurate preclinical model to evaluate toxin effects that are observed in the primary anatomical location in patients affected by CDI.[27]

The use of cancer cell lines such as Caco-2 as models to investigate biological mechanisms or preclinical models for drug testing comes with some advantages, such as ease/low cost of use and reproducible readouts. On the other hand, they suffer from homogenous responses that likely will not report the variability of responses observed in the human population. We view the inherent variability observed between hCE monolayers derived from different donors as an advantage as it has the potential to capture variability that exists in the human population. In this study, healthy transplant-grade tissue from three adult male donors varying in age and race/ethnicity was used. However, the ease of the hCE toxicity assay renders it scalable to additional donor demographics for increased representation of variable responses between humans. For example, Donor 2 appeared to be unusually sensitive to apically applied TcdA. While we cannot attribute a cause, unlike the other two donors, Donor 2 is White, and there is evidence to suggest that White patients demonstrate a higher CDI rate than patients of other races or ethnicities.[66] While we acknowledge that sample sizes would have to be increased to confirm a statistical association, this example shows that our system allows sufficiently sensitive detection of toxin responses between humans. On-going efforts to bank ISCs from female and pediatric donors will allow us to evaluate the role of sex and age on *C. difficile* toxicity. Notably, this could increase the predictive value of our system as a preclinical model and address a substantial limitation of the genetically homogenous Caco-2 cell line.

Another major strength of this model is that it allows us to consider *C. difficile* toxin effects as a multi-step process: early barrier dysfunction (initial TEER drop) which leads to increased

paracellular permeability (FITC-Dextran basal accumulation), cell rounding, and then eventual cytotoxic cell death (apoptosis) **(Fig. 7)**. Whereas currently used cell culture cytotoxicity assays that characterize cell rounding are subjective, non-standardized, and require 24 to 48 hours of incubation,[67] our platform sensitively and quantitatively captures deleterious effects of TcdA/B in as little as 2 hours. Notably, while this platform was designed to evaluate the earliest events in toxicity on differentiated epithelium, the transcriptomic data show that this platform could also be used to evaluate the impact of toxins on the stem/undifferentiated cell lineages, which to-date has not been fully characterized but has important implications for wound healing and epithelial regeneration in CDI.[68] Overall, this platform represents a flexible system and a strong experimental foundation to evaluate mechanisms of cell death or other aspects of cellular toxicities for development of new therapeutic approaches.

Beyond studying *C. difficile* toxicity, the hCE platform established here can be utilized for a wide range of translational research applications, such as evaluating the toxicity of other pathogens, modeling a leaky/inflamed hCE, and drug screening. While we tailored the hCE monolayers in this study to detect and monitor the impacts of *C. difficile* toxins A/B, our methodological approach could be applied to other microbes. For example, *Vibrio cholerae* and toxigenic *Escherichia coli*, which both are associated with life-threatening diarrhea, produce toxins that impact other colonic physiological properties such as water and ion transport that could be further characterized using the transcriptomic and experimental tools highlighted in this study.[69, 70] Additionally, given that intestinal barrier defects are associated with a variety of human pathologies and diseases, the leaky gut model could be expanded to study other disease states associated with intestinal barrier defects including IBD, celiac disease, and irritable bowel syndrome[54] to understand how these underlying conditions could potentiate disease etiology and negative effects of pathogenic microbes.

METHODS

Donor Selection

Human transplant-grade donor intestines were obtained from HonorBridge (Durham, NC) and exempted from human subjects research by the UNC Office of Human Research Ethics. Donor acceptance criteria were as follows: age 65 years or younger, brain-dead only, negative for human immunodeficiency virus, hepatitis, syphilis, tuberculosis, or COVID-19, as well as no prior history of severe abdominal injury, bowel surgery, cancer, or chemotherapy. Pancreas transplant donors were also excluded due to excision of proximal small intestinal tissue. Human intestinal tissue from three male donors (aged 29, 45, and 53 years) was used for scRNAseq.[39] Colonic tissue from a 34-year-old Hispanic male was used for bulk RNAseq, immunofluorescence staining, and monolayer studies involving FITC-conjugated dextrans. Tissue from the same donor, in addition to tissue from a 51-year-old African American male and a 29-year-old Caucasian male, was used for TcdA and TcdB apical versus basal cell surface studies comparing colon and small intestine.

Single-cell RNA Sequencing Processing and Analysis

Single-cell data was obtained from our previously published human intestinal dataset (Gene Expression Omnibus accession number: GSE185224), sequenced using an Illumina NextSeq 500 (Illumina, San Diego, CA).[39] All processing and analyses were completed using scanpy (v1.7.2).[71] Read counts were normalized to the median read depth of the data set and log-transformed.

Bulk RNA Sequencing Preparation, Processing, and Analysis

To examine the changes in gene expression as colon stem cells differentiate into late absorptive colonocytes (ACCs) in vitro, RNAseq was performed on hCE monolayers that were harvested the day after seeding onto Transwells (EM Day 1), immediately prior to switching to DM (Day 0), and on Days 2 and 4 of differentiation on Transwells. For Caco-2, RNAseq was performed using cells harvested on Day 22 of differentiation. Three technical replicates were collected at each time point, and RNA was extracted via the RNAqueous-Micro Total RNA Isolation Kit (AM1931; ThermoFisher, Waltham, MA) according to the manufacturer's protocol.

Before cDNA library preparation, RNA quality was determined by quantifying RNA integrity number (RIN), the ratio of 28s/18s RNA present, and RNA concentration in each sample. All samples used in library preparation had a RIN of at least 7. RIN was determined with the RNA 6000 Pico Kit for the Agilent 2100 Bioanalyzer. The Advanta RNA-Seq NGS Library Prep Kit for the Standard BioTools (formerly Fluidigm) Juno was used to prepare cDNA libraries for sequencing. Bulk sequencing was run on a NovaSeq 6000 instrument using one lane of an S4 v1.5 flow cell (Illumina), 2B paired-end reads, 150x read length. The Kallisto package was used to quantify transcript abundance which were pseudoaligned to human genome GRCh38. The output gene expression matrix was normalized using TMM normalization. Principal component analysis was performed with scikitlearn (v0.24.0, Rocquencourt, France).[72] Gene set enrichment analysis (GSEA) was performed with normalized bulk RNAseq data using GSEA v4.2.3[73, 74] and previously published gene signatures for colon ISC and late ACC clusters versus the rest of the colon.[39]

Collagen Hydrogel Scaffold Preparation

6-well tissue-culture plates (3516; Corning, Corning, NY) for expansion were coated with ice-cold type I rat tail collagen (354236; Corning, Corning, NY) in neutralization buffer based on an established protocol.[75] Briefly, after being incubated at 37ºC in 5% CO_2 for 1 hour, sterile tissue-culture plates were coated with 1 mL of diluted (1 mg/mL) rat-tail collagen for each well. Plates were incubated at 37ºC in 5% CO_2 for 1 hour, then 3 mL room-temperature 1X Dulbecco's phosphate-buffered saline (DPBS) (14040141; Thermo Fisher Scientific, Waltham, MA) was added onto each well. Plates were then kept overlaid with DPBS at room temperature for ≥ 2 weeks prior to use.

Primary Human Crypt Isolation and Intestinal Epithelial Stem Cell Culture

Surgical specimens of human small and large intestines were obtained from donors at HonorBridge (formerly Carolina Donor Services, Durham, NC). Crypts from desired regions (Jej, DC) of each donor were detached from the specimen as previously described[36, 37, 39] using a chelating buffer[76] composed of EDTA (2 mM), dithiothreitol (DTT, 0.5 mM, freshly added), Na_2HPO_4 (5.6 mM), KH_2PO_4 (8.0 mM), NaCl (96.2 mM), KCl (1.6 mM), sucrose (43.4 mM), D-sorbitol (54.9 mM), pH 7.4. Released crypts were expanded as a monolayer on a neutralized collagen hydrogel as described previously.[36-38]

Briefly, crypts were placed on the top of 1 mg/mL collagen hydrogels (1 ml into each well of 6-well plate) at a density of 10,000 crypts/well, overlaid with 3 mL of Expansion Media (EM) containing 10 mmol/L Y-27632 (S1049; SelleckChem, Houston, TX), and incubated at 37ºC in 5% CO_2. **See Table 1 for small intestine and colon EM formulations.** EM was used to expand the epithelial cell numbers as monolayers; media was changed the day after seeding and every 48 hours afterwards. When the cell coverage was greater than 80% (typically 4 to 6 days), the epithelium was dissociated to fragments to seed onto either 6-well tissue-culture plates coated with collagen hydrogels for continued expansion, or onto 12-well Transwell inserts (3460; Corning, Corning, NY) coated with 1% Matrigel for experiments.

Transwell Preparation and Intestinal Epithelial Stem Cell Differentiation

Briefly, 500 µL ice-cold 1% Growth Factor Reduced Matrigel (354230; Corning, Corning, NY) diluted in ice-cold DPBS was added to the apical surface of 12-well Transwell inserts. Transwell plates were then incubated at 37ºC in 5% CO_2 overnight and then rinsed 2-3 times with 1X DPBS. Dissociated intestinal epithelial stem cells that were expanded on collagen hydrogels were resuspended in 500 µL of EM per Transwell insert and seeded on the apical surface of each insert at an approximate density of 1.5×10^5 cells/cm^2. 1.5 mL of EM was added to the basal reservoir at the time of seeding. Both the apical and basal media were replaced with fresh EM the day after seeding. After sufficient cell coverage on Transwells (e.g., no visible monolayer gaps), on Day 4, Differentiation Medium (DM)[77] **(Table 1)** was used to initiate differentiation as well as during toxin experiments.

Caco-2 Cell Culture and Differentiation

Caco-2 cells (HTB-37; ATCC, Manassas, VA) were grown on a 10 cm polystyrene tissue culture-treated dish (430167; Corning, Corning, NY) in Dulbecco's Modified Eagle Media + 10% fetal bovine serum + 1% penicillin-streptomycin based on an established protocol **(Table 2)**.[78] Caco-2 media was changed every 2 days until desired confluency was reached. Two 60%

confluent 10 cm dishes were seeded onto 24 inserts in a 12-well Transwell plate coated with 30 µg/mL collagen in 1X DPBS. Spontaneous differentiation of Caco-2 monolayers was allowed to occur over 21 days, and media was changed every 2 days until the start of toxin experiments on Day 22.

C. difficile Toxins Information

Toxin A (SML1154; Sigma-Aldrich, St. Louis, MO) and Toxin B (SML1153; Sigma-Aldrich, St. Louis, MO) were reconstituted in purified water and then diluted to 30 pM, 150 pM, or 300 pM (for dose-response) in DM before adding to differentiated cells or Caco-2 on Transwell plates. These native toxins are purified from *C. difficile* strain VPI10463 (toxinotype 0) which is from Clade 1 (as opposed to Clade 2 strains for which TcdB does not appear to bind FZDs).[79] 30 pM (1X) was chosen as a clinically-relevant concentration based on ultrasensitive digital enzyme-linked immunosorbent assays (ELISAs) for TcdA and TcdB conducted on clinical specimens that tested positive for cytotoxicity.[51]

Transepithelial Electrical Resistance (TEER) Measurements

Intestinal epithelial barrier integrity was quantified via transepithelial electrical resistance (TEER) using an EVOM2™ paired with STX2 electrodes (World Precision Instruments, FL). TEER was measured daily during differentiation and every 2 hours after adding toxin for 12 hours, followed by a 24-hour timepoint. Toxin was added on DM Day 3 (DC) or DM Day 4 (jejunum). For Caco-2, TEER was measured every two days (starting day 1) and media was changed every 2 days during spontaneous differentiation. For Caco-2 TEER measurements in the presence of toxin, TcdA or TcdB was added to the apical side of Transwell inserts on Day 22.

Microscopy and Immunofluorescence Staining of Differentiated Human Colonic Epithelium

After the 24-hour timepoint, control and TcdA or TcdB-treated primary human colonic epithelial monolayers were fixed in 4% paraformaldehyde in PBS at 37ºC for 15 minutes. Cells were then permeabilized in 0.5% Triton-X100 at room temperature for 20 minutes, followed by blocking with 3% BSA in PBS for 1 hour at room temperature. The cells were treated with primary antibody against cleaved-caspase 3 (1:300, 9661S; Cell Signaling Technology, Danvers, MA) and incubated at 4ºC overnight. The cells were then washed with a rinse solution consisting of 0.1% BSA, 0.2% Triton-X100, and 0.05% Tween-20, then incubated with Alexa Fluor 488-conjugated donkey anti-rabbit antibody (1:500, 711-545-152; Jackson ImmunoResearch, West Grove, PA) and bisbenzimide H 33258 (1:1000, B1155; Sigma-Aldrich-Aldrich, St. Louis, MO) diluted in 3% BSA in PBS for 1 hour at room temperature. Cells were washed in 1X DPBS twice prior to microscopy. Images were captured using an LSM700 confocal microscope (Zeiss, Jena, Germany) 10X objective and ZEN 2011 acquisition software, with post-acquisition processing using FIJI.[80]

Basal Fluorescent Dextran Quantification and Diclofenac Permeability Assays

Permeability assays were conducted as previously described.[36] Briefly, 250 kDa FITC-Dextran (FD250S; Sigma-Aldrich, St. Louis, MO) was chosen to mimic the size of TcdB (270 kDa). FITC-Dextran was diluted to 1 µM in DM and added to the apical side of 12-well Transwell inserts with or without 30 pM TcdB. Basal media (100 µL) was collected every 2 hours for 12 hours and replaced with an equivalent volume of DM (or DM with TcdB), followed by a 24-hour timepoint.

Basal collections were added to a 96-well microplate for fluorescence-based assays (M33089; ThermoFisher, Waltham, MA). FITC-associated fluorescence was measured by CLARIOstar Plus Microplate Reader (BMG Labtech, Ortenberg, Germany) after excitation at 483 nm and detection at 530 nm. Relative fluorescence units were converted to picomoles using a standard curve. Diclofenac sodium salt (157660; MP Biomedicals, Solon, OH) was reconstituted in DMSO and diluted to 1 mM in DM containing FITC-Dextran with or without TcdB.

Statistics

For comparing gene expression in scRNAseq data **(Fig. 2B, D, and F)**, significance was calculated by negative binomial regression with the diffxpy python package (v0.7.4) using the Wald test and Benjamini-Hochberg correction. TEER values at each day of DM (or Caco-2 media) were compared against TEER at D0 (or Caco-2 Day 1) using a 1-way repeated measures ANOVA with Bonferroni correction **(Fig. 4C-E)**. Experimental TEER values were compared against vehicle control for dose-response data **(Fig. 5B)** using the Kruskal-Wallis test with Benjamini-Hochberg correction due to data non-normality, and in **Fig. 5C, D, and F** using a 1-way ANOVA followed by Dunnett's multiple comparisons test**.** 1-way ANOVA followed by Dunnett's multiple comparisons tests were used to compare FITC-Dextran permeability between control and experimental groups **(Fig. 6)**.

Access to Data: All authors had access to all the data and have reviewed and approved the final manuscript.

ACKNOWLEDGEMENTS

First and foremost, thank you to the anonymous organ donors, their families, and HonorBridge (Durham, NC) for providing the intestinal tissue samples used in this study. Schematics in Figures 1A, 3A, 4A, 4B, 5A, 6, and 7 were created using BioRender. Thank you to the UNC High-Throughput Sequencing Facility and the CGIBD Advanced Analytics Core, especially Gabrielle Cannon, for RNA-seq data. Thank you to Casey Theriot, Rita Tamayo, Carly Catella, Carol Hall, Sudeep Sarma, Nick Markham, and Aadra Bhatt for useful discussions and James Stroud, Nathan Kohn, and Yunan Hu for support with TEER measurements.

FIGURE LEGENDS

Figure 1. Single-cell transcriptomics demonstrates variations in expression patterns and magnitude of *C. difficile* toxin receptor genes across all intestinal epithelial cell lineages. (A) Healthy human organ donor demographic information for single-cell RNAseq data. **(B)** Dotplot showing the fraction of expressing cells (circle size) and magnitude (color) of expression for known *C. difficile* toxin receptor genes across all small intestinal and colonic epithelial cell lineages. SI, Small Intestine; ISC, Intestinal Stem Cell; TA, Transit-Amplifying; AE, Absorptive Enterocyte; Interm., Intermediate; Sec. Prog, Secretory Progenitor; EEC, Enteroendocrine Cell; FAE, Follicle-Associated Epithelium; C, Colon; ACC, Absorptive Colonocyte.

Figure 2. Single-cell RNAseq survey of *C. difficile*-toxin relevant genes reveals organ and lineage variability. **(A)** Dotplots comparing *C. difficile* toxin receptor genes across small intestinal and colonic epithelial regions in stem cells (left) and mature absorptive cells (right) and **(B)** corresponding significance bar graphs. **(C)** Dotplots comparing Rho GTPase family genes by intestinal region in stem cells (left) and mature absorptive cells (right) and **(D)** corresponding significance bar graphs. **(E)** Dotplots comparing curated tight junction genes by intestinal region in stem cells (left) and mature absorptive cells (right) and **(F)** corresponding significance bar graphs. All bar graphs show fold-change in reads per 10,000 genes (RP10K) across 3 donors for colon normalized to small intestine, mean ± SD. *$q < 0.05$, **$q < 0.01$, ***$q < 0.001$, ****$q < 0.0001$. Duo, Duodenum; Jej, Jejunum; Ile, Ileum; AC, Ascending Colon; TC, Transverse Colon; DC, Descending Colon.

Figure 3. Bulk RNAseq reveals Caco-2 monolayers remain stem-like and hCE monolayers mature over time to mimic in vivo late absorptive colonocytes. (A) Schematic of expansion and differentiation of human colonic epithelial (hCE) monolayers on Transwells. **(B)** Principal component analysis of sequenced transcriptomes. Matrix plots comparing hCE and Caco-2 cells (n = 3 Transwells each) using top 30 differentially expressed genes (DEGs) for **(C)** colon intestinal stem cells (ISCs) and **(D)** late absorptive colonocytes (ACCs) versus the rest of the colon, and **(E)** S-phase and G2/M-phase genes in descending colon (DC) vs. Caco-2 cell monolayers. Gene set enrichment analysis for DC in differentiation media (DM) Day 4 (red) and differentiated Caco-2 cells (blue) using gene sets consisting of **(F)** all in vivo colon ISC DEGs, and **(G)** all in vivo late ACC DEGs.

Figure 4. Human colonic epithelial cells exhibit elevated TEER during differentiation compared to Caco-2 or small intestinal epithelial monolayers. (A) Healthy human organ donor demographic information for transepithelial electrical resistance (TEER) assays. **(B)** Schematic and timeline for TEER (i.e., ionic conductance) measurements during differentiation of human intestinal epithelial monolayers. Monolayer TEER measurements for **(C)** human colonic epithelium, achieving a tight epithelial barrier within 1-day differentiation media (DM) exposure (N = 3 donors, n = 15 Transwells/donor for all days except n = 3 Transwells/donor for Day 4 DM), **(D)** Caco-2 cells (n = 21 Transwells), and **(E)** human small intestinal epithelium (N = 3 donors, n = 15 Transwells/donor). TEER values were compared against TEER at DM D0 (or Caco-2 Day 1) using

a 1-way repeated measures ANOVA with Bonferroni correction. Each data point represents the mean ± SD. *$p < 0.05$, **$p < 0.01$, ***$p < 0.001$, ****$p < 0.0001$.

Figure 5. Basal *C. difficile* TcdA/B exposure induces more rapid cytotoxicity than apical toxin exposure in differentiated human colonic epithelium. (A) After seeding cells on Transwells in expansion media (EM) and switching to differentiation media (DM), TcdA or TcdB was added on DM Day 3 (D3) at t = 0 for 24 hours. **(B)** Dose-response of differentiated human colonic epithelium (hCE) to apical TcdA or TcdB at 30 pM (1X), 150 pM (5X), or 300 pM (10X); n = 4 Transwells, mean ± SD. TEER is reported as % of initial value (at t = 0). Kruskal-Wallis test with Benjamini-Hochberg correction was used. *$q < 0.05$, **$q < 0.01$, ***$q < 0.001$. Monolayer TEER measurements for differentiated **(C)** hCE and **(D)** human jejunal epithelium. **(E)** Representative immunofluorescence staining (CC3, cleaved-caspase 3; Nuclei, bisbenzimide) and brightfield image (Control) of fixed apical/basal TcdA or TcdB-treated hCE, 24 hours post-treatment. Images were taken using a Zeiss LSM710 confocal 10X objective and ZEN 2011 acquisition software, with post-acquisition processing using FIJI. All scalebars = 50 µm. **(F)** TEER measurements for differentiated Caco-2 monolayers after apical or basal addition of TcdA or TcdB. For **C, D, and F**, toxins were added to DM at 1X = 30 pM; N = 3 donors for human colon and jejunum, and n = 3 Transwells, mean ± SD. 1-way ANOVA followed by Dunnett's multiple comparisons test were used. *$p < 0.05$, **$p < 0.01$, ***$p < 0.001$, ****$p < 0.0001$.

Figure 6. A leaky human colonic epithelium induced by diclofenac reduces apical barrier protection from TcdB. Schematic showing TcdB-sized FITC-Dextran (250 kDa) added to the apical surface of Transwells with or without differentiated human colonic epithelium (hCE), +/- TcdB, and +/- diclofenac and resulting permeability (n = 3 Transwells). Permeability data shows cumulative FITC-Dextran (pmol) transported from apical to basal compartments of Transwells. Tx = treatment. Each data point represents the mean ± SD. 1-way ANOVA followed by Dunnett's multiple comparisons test were used. *$p < 0.05$, **$p < 0.01$, ***$p < 0.001$, ****$p < 0.0001$.

Figure 7. Human colonic epithelial cell platform detects early evidence of *C. difficile* toxicity. TcdA and TcdB enzymatic toxins are secreted by *C. difficile*, bind to host receptors, enter cells via endocytosis, and inactivate Rho-family GTPases by monoglucosylation. This results in early barrier injury, increased paracellular permeability to toxins, cell rounding, and eventual apoptosis.

REFERENCES

1. Kordus SL, Thomas AK, Lacy DB. Clostridioides difficile toxins: mechanisms of action and antitoxin therapeutics. Nature Reviews. Microbiology 2021.
2. Zhang S, Palazuelos-Munoz S, Balsells EM, et al. Cost of hospital management of Clostridium difficile infection in United States—a meta-analysis and modelling study. BMC Infectious Diseases 2016;16.
3. Nitzan O. Clostridium difficile and inflammatory bowel disease: Role in pathogenesis and implications in treatment. World Journal of Gastroenterology 2013;19:7577.
4. Johnson S, Lavergne V, Skinner AM, et al. Clinical Practice Guideline by the Infectious Diseases Society of America (IDSA) and Society for Healthcare Epidemiology of America (SHEA): 2021 Focused Update Guidelines on Management of Clostridioides difficile Infection in Adults. Clin Infect Dis 2021;73:e1029-e1044.
5. Peng Z, Jin D, Kim HB, et al. Update on Antimicrobial Resistance in Clostridium difficile: Resistance Mechanisms and Antimicrobial Susceptibility Testing. Journal of Clinical Microbiology 2017;55:1998-2008.
6. Kelly CP, Lamont JT. Clostridium difficile— More Difficult Than Ever. New England Journal of Medicine 2008;359:1932-1940.
7. Louie TJ, Miller MA, Mullane KM, et al. Fidaxomicin versus Vancomycin for Clostridium difficile Infection. New England Journal of Medicine 2011;364:422-431.
8. Kuehne SA, Collery MM, Kelly ML, et al. Importance of Toxin A, Toxin B, and CDT in Virulence of an Epidemic Clostridium difficile Strain. The Journal of Infectious Diseases 2014;209:83-86.
9. Martinez-Melendez A, Cruz-Lopez F, Morfin-Otero R, et al. An Update on Clostridioides difficile Binary Toxin. Toxins (Basel) 2022;14.
10. Voth DE, Ballard JD. Clostridium difficile toxins: mechanism of action and role in disease. Clinical Microbiology Reviews 2005;18:247-263.
11. Orrell KE, Melnyk RA. Large Clostridial Toxins: Mechanisms and Roles in Disease. Microbiol Mol Biol Rev 2021;85:e0006421.
12. Orrell KE, Zhang Z, Sugiman-Marangos SN, et al. Clostridium difficile toxins A and B: Receptors, pores, and translocation into cells. Critical Reviews in Biochemistry and Molecular Biology 2017;52:461-473.
13. Aktories K, Schwan C, Jank T. Clostridium difficile Toxin Biology. Annual Review of Microbiology 2017;71:281-307.
14. Hecht G, Pothoulakis C, LaMont JT, et al. Clostridium difficile toxin A perturbs cytoskeletal structure and tight junction permeability of cultured human intestinal epithelial monolayers. The Journal of Clinical Investigation 1988;82:1516-1524.
15. Hecht G, Koutsouris A, Pothoulakis C, et al. Clostridium difficile toxin B disrupts the barrier function of T84 monolayers. Gastroenterology 1992;102:416-423.
16. Du T, Alfa MJ. Translocation of Clostridium difficile Toxin B across Polarized Caco-2 Cell Monolayers Is Enhanced by Toxin A. Canadian Journal of Infectious Diseases 2004;15:83-88.
17. Rothman SW, Brown JE, Diecidue A, et al. Differential cytotoxic effects of toxins A and B isolated from Clostridium difficile. Infection and Immunity 1984;46:324-331.

18. Sutton PA, Li S, Webb J, et al. Essential role of toxin A in C. difficile 027 and reference strain supernatant-mediated disruption of Caco-2 intestinal epithelial barrier function. Clinical and Experimental Immunology 2008;153:439-447.
19. Carter GP, Rood JI, Lyras D. The role of toxin A and toxin B in Clostridium difficile-associated disease: Past and present perspectives. Gut microbes 2010;1:58-64.
20. Kleiveland CR. Co-cultivation of Caco-2 and HT-29MTX: Springer International Publishing, 2015:135-140.
21. Lea T. Caco-2 Cell Line. In: Verhoeckx K, Cotter P, López-Expósito I, Kleiveland C, Lea T, Mackie A, Requena T, Swiatecka D, Wichers H, eds. The Impact of Food Bioactives on Health: in vitro and ex vivo models. Cham (CH): Springer, 2015.
22. Chaves-Olarte E, Weidmann M, Eichel-Streiber C, et al. Toxins A and B from Clostridium difficile differ with respect to enzymatic potencies, cellular substrate specificities, and surface binding to cultured cells. The Journal of Clinical Investigation 1997;100:1734-1741.
23. Donta ST, Sullivan N, Wilkins TD. Differential Effects of Clostridium difficile Toxins on Tissue-Cultured Cells. Journal of Clinical Microbiology 1982;15:1157-1158.
24. Leslie JL, Huang S, Opp JS, et al. Persistence and toxin production by Clostridium difficile within human intestinal organoids result in disruption of epithelial paracellular barrier function. Infection and Immunity 2015;83:138-145.
25. Engevik MA, Danhof HA, Chang-Graham AL, et al. Human intestinal enteroids as a model of Clostridioides difficile-induced enteritis. American Journal of Physiology. Gastrointestinal and Liver Physiology 2020;318:G870-G888.
26. Spence JR, Mayhew CN, Rankin SA, et al. Directed differentiation of human pluripotent stem cells into intestinal tissue in vitro. Nature 2011;470:105-109.
27. Fordtran JS. Colitis Due to Clostridium Difficile Toxins: Underdiagnosed, Highly Virulent, and Nosocomial. Baylor University Medical Center Proceedings 2006;19:3-12.
28. Na X, Kim H, Moyer MP, et al. gp96 Is a Human Colonocyte Plasma Membrane Binding Protein for Clostridium difficile Toxin A. Infection and Immunity 2008;76:2862-2871.
29. Schottelndreier D, Langejurgen A, Lindner R, et al. Low Density Lipoprotein Receptor-Related Protein-1 (LRP1) Is Involved in the Uptake of Clostridioides difficile Toxin A and Serves as an Internalizing Receptor. Front Cell Infect Microbiol 2020;10:565465.
30. Marzolo M-P, Yuseff MI, Retamal C, et al. Differential Distribution of Low-Density Lipoprotein-Receptor-Related Protein (LRP) and Megalin in Polarized Epithelial Cells is Determined by Their Cytoplasmic Domains. Traffic 2003;4:273-288.
31. Tao L, Zhang J, Meraner P, et al. Frizzled proteins are colonic epithelial receptors for C. difficile toxin B. Nature 2016;538:350-355.
32. Chen P, Tao L, Wang T, et al. Structural basis for recognition of frizzled proteins by Clostridium difficile toxin B. Science 2018;360:664-669.
33. Vincan E, Darcy PK, Farrelly CA, et al. Frizzled-7 dictates three-dimensional organization of colorectal cancer cell carcinoids. Oncogene 2007;26:2340-52.
34. LaFrance ME, Farrow MA, Chandrasekaran R, et al. Identification of an epithelial cell receptor responsible for Clostridium difficile TcdB-induced cytotoxicity. Proc Natl Acad Sci U S A 2015;112:7073-8.

35. Xie L, Fletcher RB, Bhatia D, et al. Robust Colonic Epithelial Regeneration and Amelioration of Colitis via FZD-Specific Activation of Wnt Signaling. Cellular and Molecular Gastroenterology and Hepatology 2022.
36. Gomez-Martinez I, Bliton RJ, Breau KA, et al. A planar culture model of human absorptive enterocytes reveals metformin increases fatty acid oxidation and export. Cell Mol Gastroenterol Hepatol 2022.
37. Breau KA, Ok MT, Gomez-Martinez I, et al. Efficient transgenesis and homology-directed gene targeting in monolayers of primary human small intestinal and colonic epithelial stem cells. Stem Cell Reports 2022.
38. Wang Y, DiSalvo M, Gunasekara DB, et al. Self-renewing Monolayer of Primary Colonic or Rectal Epithelial Cells. Cellular and Molecular Gastroenterology and Hepatology 2017;4:165-182.e7.
39. Burclaff J, Bliton RJ, Breau KA, et al. A proximal-to-distal survey of healthy adult human small intestine and colon epithelium by single-cell transcriptomics. Cellular and Molecular Gastroenterology and Hepatology 2022.
40. Pothoulakis C, Gilbert RJ, Cladaras C, et al. Rabbit sucrase-isomaltase contains a functional intestinal receptor for Clostridium difficile toxin A. Journal of Clinical Investigation 1996;98:641-649.
41. Papatheodorou P, Carette JE, Bell GW, et al. Lipolysis-stimulated lipoprotein receptor (LSR) is the host receptor for the binary toxin Clostridium difficile transferase (CDT). Proc Natl Acad Sci U S A 2011;108:16422-7.
42. Van Beers EH, Buller HA, Grand RJ, et al. Intestinal brush border glycohydrolases: structure, function, and development. Crit Rev Biochem Mol Biol 1995;30:197-262.
43. Just I, Selzer J, Wilm M, et al. Glucosylation of Rho proteins by Clostridium difficile toxin B. Nature 1995;375:500-503.
44. Just I, Wilm M, Selzer J, et al. The Enterotoxin from Clostridium difficile (ToxA) Monoglucosylates the Rho Proteins. Journal of Biological Chemistry 1995;270:13932-13936.
45. Just I, Fritz G, Aktories K, et al. Clostridium difficile toxin B acts on the GTP-binding protein Rho. Journal of Biological Chemistry 1994;269:10706-10712.
46. Vancamelbeke M, Vanuytsel T, Farré R, et al. Genetic and Transcriptomic Bases of Intestinal Epithelial Barrier Dysfunction in Inflammatory Bowel Disease. Inflammatory Bowel Diseases 2017;23:1718-1729.
47. Suzuki T. Regulation of the intestinal barrier by nutrients: The role of tight junctions. Animal Science Journal 2020;91.
48. Kowalczyk MS, Tirosh I, Heckl D, et al. Single-cell RNA-seq reveals changes in cell cycle and differentiation programs upon aging of hematopoietic stem cells. Genome Research 2015;25:1860-1872.
49. Srinivasan B, Kolli AR, Esch MB, et al. TEER Measurement Techniques for In Vitro Barrier Model Systems. SLAS Technology 2015;20:107-126.
50. Van Der Flier LG, Clevers H. Stem Cells, Self-Renewal, and Differentiation in the Intestinal Epithelium. Annual Review of Physiology 2009;71:241-260.

51. Song L, Zhao M, Duffy DC, et al. Development and Validation of Digital Enzyme-Linked Immunosorbent Assays for Ultrasensitive Detection and Quantification of Clostridium difficile Toxins in Stool. Journal of Clinical Microbiology 2015;53:3204-3212.
52. Chandrasekaran R, Lacy DB. The role of toxins in Clostridium difficile infection. FEMS Microbiology Reviews 2017;41:723-750.
53. Riegler M, Sedivy R, Pothoulakis C, et al. Clostridium difficile toxin B is more potent than toxin A in damaging human colonic epithelium in vitro. Journal of Clinical Investigation 1995;95:2004-2011.
54. Odenwald MA, Turner JR. Intestinal Permeability Defects: Is It Time to Treat? Clinical Gastroenterology and Hepatology 2013;11:1075-1083.
55. Gibson GR. Colitis Induced by Nonsteroidal Anti-inflammatory Drugs. Archives of Internal Medicine 1992;152:625.
56. Suissa D, Delaney JAC, Dial S, et al. Non-steroidal anti-inflammatory drugs and the risk of Clostridium difficile-associated disease. British Journal of Clinical Pharmacology 2012;74:370-375.
57. Permpalung N, Upala S, Sanguankeo A, et al. Association between NSAIDs and Clostridium difficile-Associated Diarrhea: A Systematic Review and Meta-Analysis. Canadian Journal of Gastroenterology and Hepatology 2016;2016:1-9.
58. Bhatt AP, Gunasekara DB, Speer J, et al. Nonsteroidal Anti-Inflammatory Drug-Induced Leaky Gut Modeled Using Polarized Monolayers of Primary Human Intestinal Epithelial Cells. ACS Infect Dis 2018;4:46-52.
59. Niu X, De Graaf IAM, Langelaar-Makkinje M, et al. Diclofenac toxicity in human intestine ex vivo is not related to the formation of intestinal metabolites. Archives of Toxicology 2015;89:107-119.
60. Kararli TT. Comparison of the gastrointestinal anatomy, physiology, and biochemistry of humans and commonly used laboratory animals. Biopharmaceutics & Drug Disposition 1995;16:351-380.
61. McConnell EL, Fadda HM, Basit AW. Gut instincts: explorations in intestinal physiology and drug delivery. Int J Pharm 2008;364:213-26.
62. Dong L, Tomassen MM, Ariëns RMC, et al. Clostridioides difficile toxin A-mediated Caco-2 cell barrier damage was attenuated by insect-derived fractions and corresponded to increased gene transcription of cell junctional and proliferation proteins. Food & function 2021;12:9248-9260.
63. Pietrangeli P, Corpetti C, Seguella L, et al. Lathyrus sativus diamine oxidase reduces Clostridium difficile toxin A-induced toxicity in Caco-2 cells by rescuing RhoA-GTPase and inhibiting pp38-MAPK/NF-κB/HIF-1α activation. Phytotherapy Research 2021;35:415-423.
64. Natoli M, Leoni BD, D'Agnano I, et al. Good Caco-2 cell culture practices. Toxicology in Vitro 2012;26:1243-1246.
65. Hidalgo IJ, Raub TJ, Borchardt RT. Characterization of the Human Colon Carcinoma Cell Line (Caco-2) as a Model System for Intestinal Epithelial Permeability. Gastroenterology 1989;96:736-749.

66. Mao EJ, Kelly CR, Machan JT. Racial Differences in Clostridium difficile Infection Rates Are Attributable to Disparities in Health Care Access. Antimicrobial Agents and Chemotherapy 2015;59:6283-6287.
67. Pollock NR. Ultrasensitive Detection and Quantification of Toxins for Optimized Diagnosis of Clostridium difficile Infection. Journal of Clinical Microbiology 2016;54:259-264.
68. Mileto SJ, Jardé T, Childress KO, et al. Clostridioides difficile infection damages colonic stem cells via TcdB, impairing epithelial repair and recovery from disease. Proceedings of the National Academy of Sciences of the United States of America 2020;117:8064-8073.
69. Speelman P, Butler T, Kabir I, et al. Colonic Dysfunction During Cholera Infection. Gastroenterology 1986;91:1164-1170.
70. Field M. Intestinal ion transport and the pathophysiology of diarrhea. 2003;111:931-943.
71. Wolf FA, Angerer P, Theis FJ. SCANPY: large-scale single-cell gene expression data analysis. Genome Biology 2018;19.
72. Pedregosa F, Varoquaux G, Michel V, et al. Scikit-learn: Machine learning in Python. the Journal of machine Learning research 2011;12:2825-2830.
73. Subramanian A, Tamayo P, Mootha VK, et al. Gene set enrichment analysis: A knowledge-based approach for interpreting genome-wide expression profiles. Proceedings of the National Academy of Sciences 2005;102:15545-15550.
74. Mootha VK, Lindgren CM, Eriksson K-F, et al. PGC-1α-responsive genes involved in oxidative phosphorylation are coordinately downregulated in human diabetes. Nature Genetics 2003;34:267-273.
75. Hinman SS, Wang Y, Kim R, et al. In vitro generation of self-renewing human intestinal epithelia over planar and shaped collagen hydrogels. Nature Protocols 2021;16:352-382.
76. Sato T, Stange DE, Ferrante M, et al. Long-term expansion of epithelial organoids from human colon, adenoma, adenocarcinoma, and Barrett's epithelium. Gastroenterology 2011;141:1762-1772.
77. Wang Y, Kim R, Hwang S-HJ, et al. Analysis of Interleukin 8 Secretion by a Stem-Cell-Derived Human-Intestinal-Epithelial-Monolayer Platform. Analytical Chemistry 2018;90:11523-11530.
78. Maciel AAFL, Oriá RB, Braga-Neto MB, et al. Role of retinol in protecting epithelial cell damage induced by Clostridium difficile toxin A. Toxicon 2007;50:1027-1040.
79. Henkel D, Tatge H, Schöttelndreier D, et al. Receptor Binding Domains of TcdB from Clostridioides difficile for Chondroitin Sulfate Proteoglycan-4 and Frizzled Proteins Are Functionally Independent and Additive. Toxins 2020;12:736.
80. Schindelin J, Arganda-Carreras I, Frise E, et al. Fiji: an open-source platform for biological-image analysis. Nature Methods 2012;9:676-682.

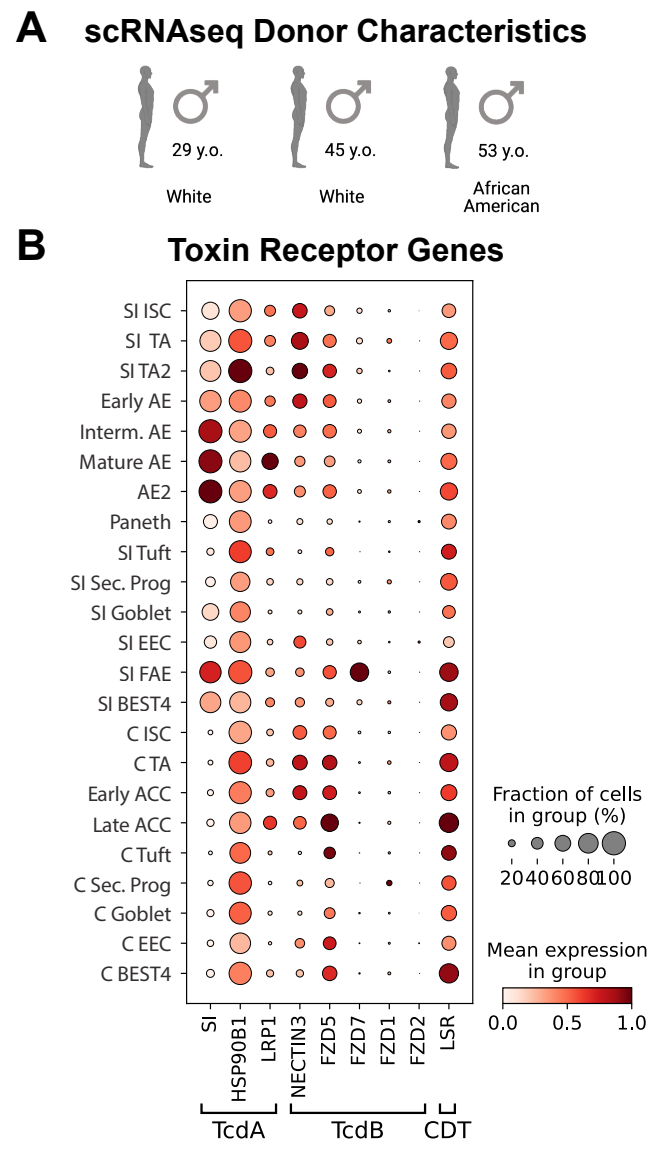
A
scRNAseq Donor Characteristics
29 y.o.
White
45 y.o.
White
53 y.o.
African American
B
Toxin Receptor Genes
SI ISC
SI TA
SI TA2
Early AE
Interm. AE
Mature AE
AE2
Paneth
SI Tuft
SI Sec. Prog
SI Goblet
SI EEC
SI FAE
SI BEST4
C ISC
C TA
Early ACC
Late ACC
C Tuft
C Sec. Prog
C Goblet
C EEC
C BEST4
SI
HSP90B1
LRP1
NECTIN3
FZD5
FZD7
FZD1
FZD2
LSR
TcdA
TcdB
CDT
Fraction of cells in group (%)
20
40
60
80
100
Mean expression in group
0.0
0.5
1.0

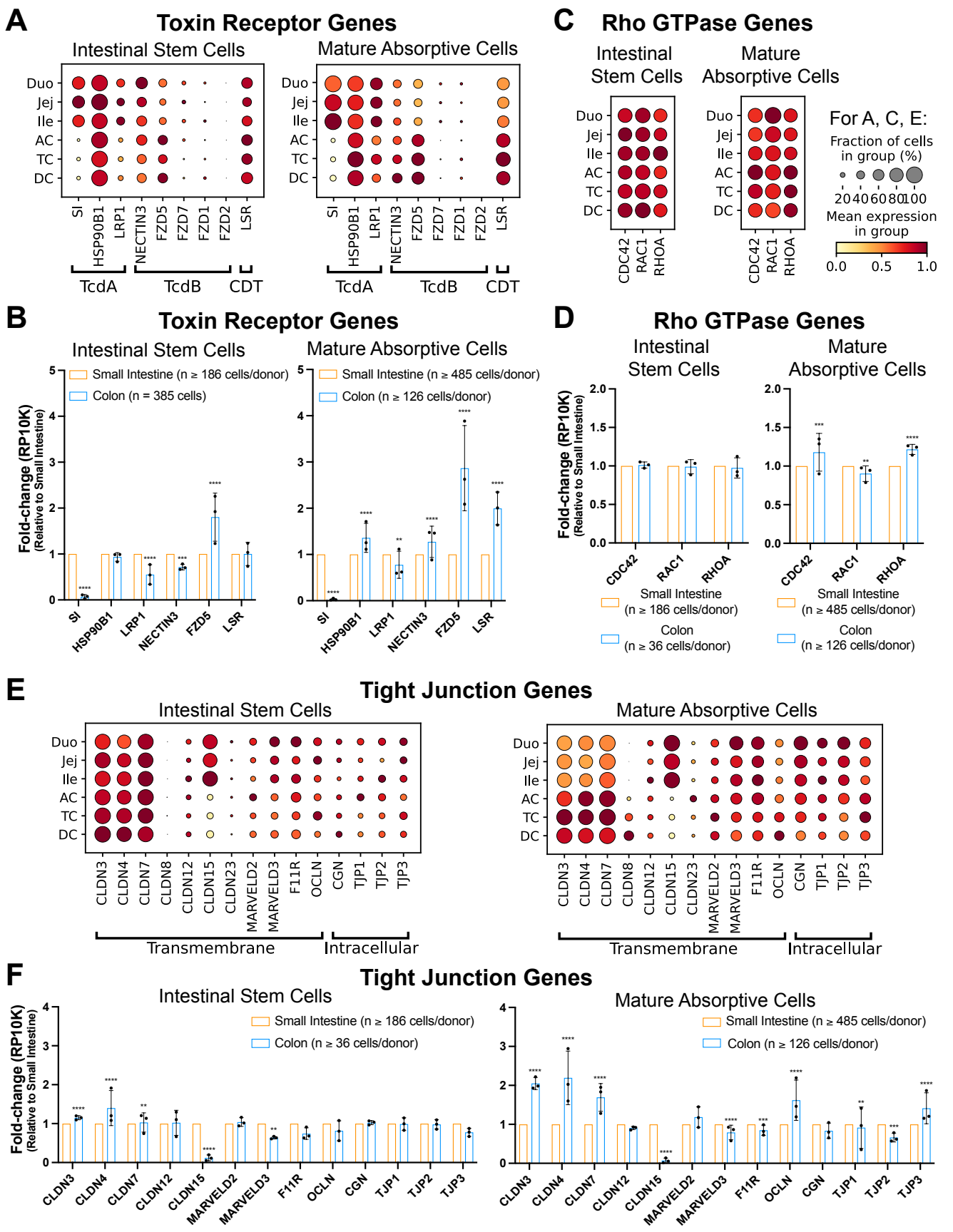
A
Toxin Receptor Genes
Intestinal Stem Cells
Mature Absorptive Cells
Duo
Jej
Ile
AC
TC
DC
SI
HSP90B1
LRP1
NECTIN3
FZD5
FZD7
FZD1
FZD2
LSR
TcdA
TcdB
CDT
C
Rho GTPase Genes
Intestinal Stem Cells
Mature Absorptive Cells
CDC42
RAC1
RHOA
For A, C, E:
Fraction of cells in group (%)
20 40 60 80 100
Mean expression in group
0.0 0.5 1.0
B
Toxin Receptor Genes
Intestinal Stem Cells
Mature Absorptive Cells
Small Intestine (n ≥ 186 cells/donor)
Colon (n = 385 cells)
Small Intestine (n ≥ 485 cells/donor)
Colon (n ≥ 126 cells/donor)
Fold-change (RP10K)
(Relative to Small Intestine)
D
Rho GTPase Genes
Intestinal Stem Cells
Mature Absorptive Cells
Small Intestine (n ≥ 186 cells/donor)
Colon (n ≥ 36 cells/donor)
Small Intestine (n ≥ 485 cells/donor)
Colon (n ≥ 126 cells/donor)
E
Tight Junction Genes
Intestinal Stem Cells
Mature Absorptive Cells
CLDN3
CLDN4
CLDN7
CLDN8
CLDN12
CLDN15
CLDN23
MARVELD2
MARVELD3
F11R
OCLN
CGN
TJP1
TJP2
TJP3
Transmembrane
Intracellular
F
Tight Junction Genes
Intestinal Stem Cells
Mature Absorptive Cells
Small Intestine (n ≥ 186 cells/donor)
Colon (n ≥ 36 cells/donor)
Small Intestine (n ≥ 485 cells/donor)
Colon (n ≥ 126 cells/donor)
Fold-change (RP10K)
(Relative to Small Intestine)

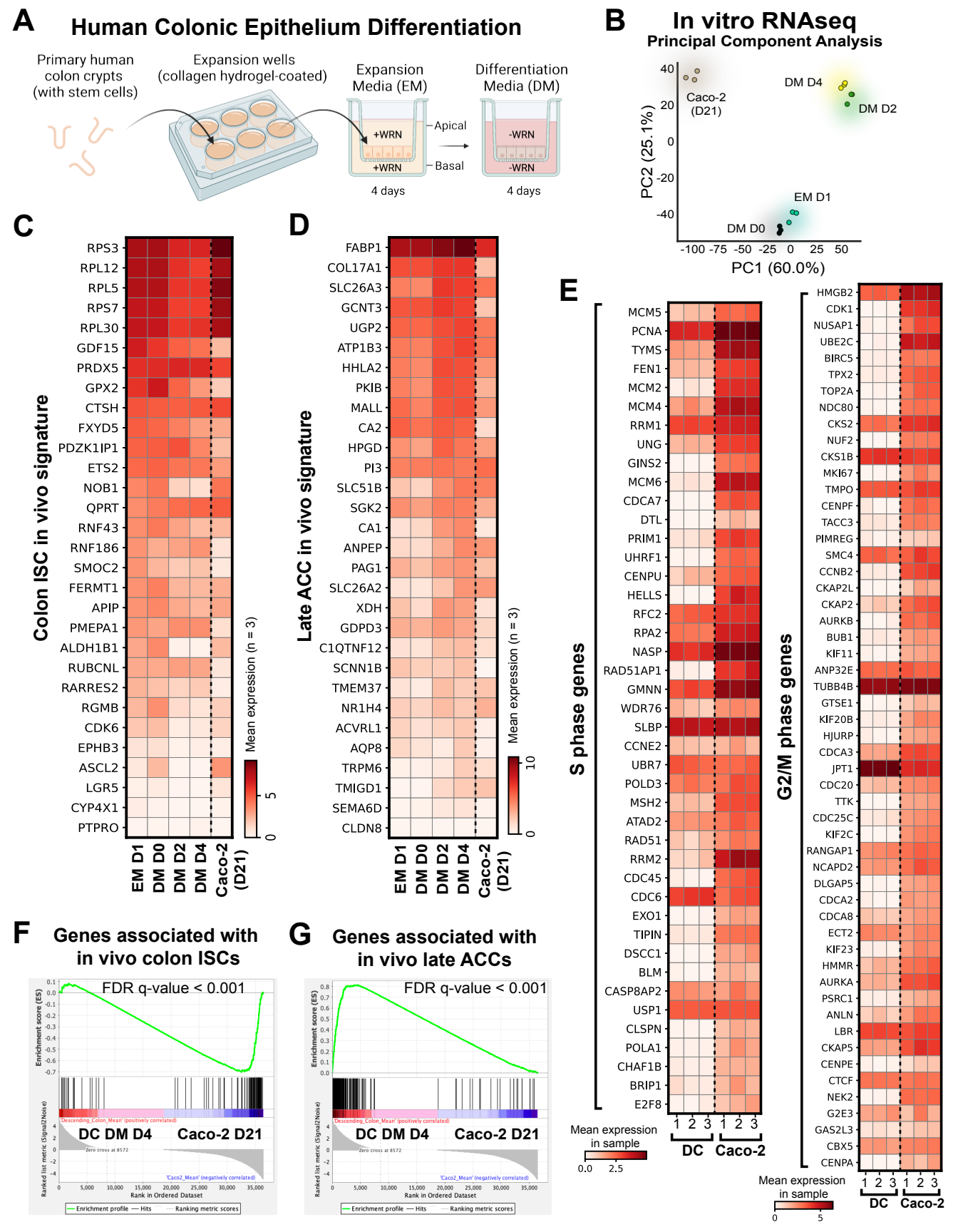
A
Human Colonic Epithelium Differentiation
Primary human colon crypts (with stem cells)
Expansion wells (collagen hydrogel-coated)
Expansion Media (EM)
Differentiation Media (DM)
+WRN
+WRN
-WRN
-WRN
Apical
Basal
4 days
4 days
B
In vitro RNAseq
Principal Component Analysis
Caco-2 (D21)
DM D4
DM D2
EM D1
DM D0
PC2 (25.1%)
PC1 (60.0%)
C
Colon ISC in vivo signature
RPS3
RPL12
RPL5
RPS7
RPL30
GDF15
PRDX5
GPX2
CTSH
FXYD5
PDZK1IP1
ETS2
NOB1
QPRT
RNF43
RNF186
SMOC2
FERMT1
APIP
PMEPA1
ALDH1B1
RUBCNL
RARRES2
RGMB
CDK6
EPHB3
ASCL2
LGR5
CYP4X1
PTPRO
Mean expression (n = 3)
EM D1
DM D0
DM D2
DM D4
Caco-2 (D21)
D
Late ACC in vivo signature
FABP1
COL17A1
SLC26A3
GCNT3
UGP2
ATP1B3
HHLA2
PKIB
MALL
CA2
HPGD
PI3
SLC51B
SGK2
CA1
ANPEP
PAG1
SLC26A2
XDH
GDPD3
C1QTNF12
SCNN1B
TMEM37
NR1H4
ACVRL1
AQP8
TRPM6
TMIGD1
SEMA6D
CLDN8
Mean expression (n = 3)
EM D1
DM D0
DM D2
DM D4
Caco-2 (D21)
E
S phase genes
MCM5
PCNA
TYMS
FEN1
MCM2
MCM4
RRM1
UNG
GINS2
MCM6
CDCA7
DTL
PRIM1
UHRF1
CENPU
HELLS
RFC2
RPA2
NASP
RAD51AP1
GMNN
WDR76
SLBP
CCNE2
UBR7
POLD3
MSH2
ATAD2
RAD51
RRM2
CDC45
CDC6
EXO1
TIPIN
DSCC1
BLM
CASP8AP2
USP1
CLSPN
POLA1
CHAF1B
BRIP1
E2F8
G2/M phase genes
HMGB2
CDK1
NUSAP1
UBE2C
BIRC5
TPX2
TOP2A
NDC80
CKS2
NUF2
CKS1B
MKI67
TMPO
CENPF
TACC3
PIMREG
SMC4
CCNB2
CKAP2L
CKAP2
AURKB
BUB1
KIF11
ANP32E
TUBB4B
GTSE1
KIF20B
HJURP
CDCA3
JPT1
CDC20
TTK
CDC25C
KIF2C
RANGAP1
NCAPD2
DLGAP5
CDCA2
CDCA8
ECT2
KIF23
HMMR
AURKA
PSRC1
ANLN
LBR
CKAP5
CENPE
CTCF
NEK2
G2E3
GAS2L3
CBX5
CENPA
Mean expression in sample
DC
Caco-2
F
Genes associated with in vivo colon ISCs
FDR q-value < 0.001
DC DM D4
Caco-2 D21
Enrichment score (ES)
Ranked list metric (Signal2Noise)
Rank in Ordered Dataset
Enrichment profile
Hits
Ranking metric scores
G
Genes associated with in vivo late ACCs
FDR q-value < 0.001
DC DM D4
Caco-2 D21
Enrichment score (ES)
Ranked list metric (Signal2Noise)
Rank in Ordered Dataset
Enrichment profile
Hits
Ranking metric scores

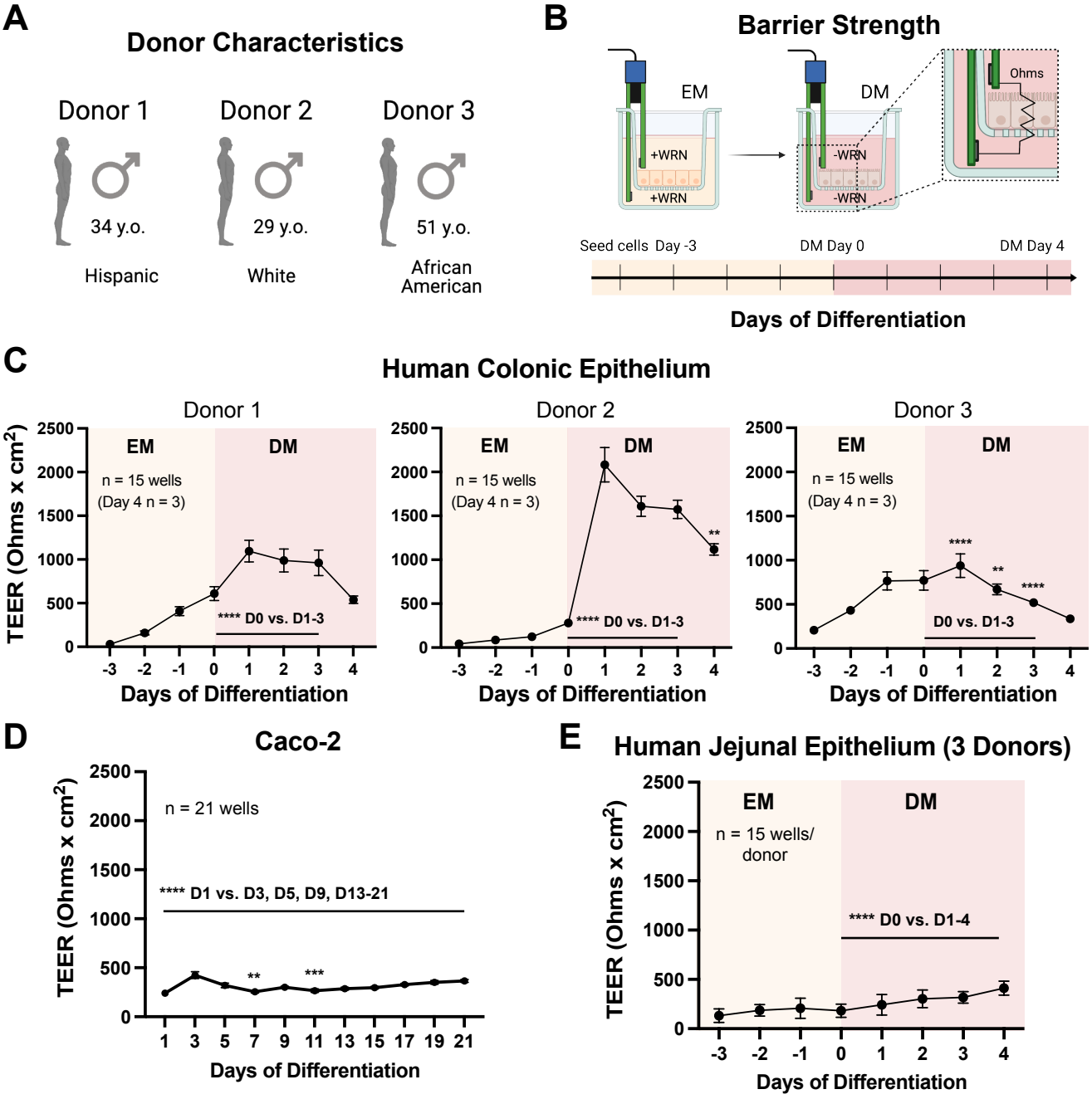
A
Donor Characteristics
Donor 1
34 y.o.
Hispanic
Donor 2
29 y.o.
White
Donor 3
51 y.o.
African American
B
Barrier Strength
EM
+WRN
+WRN
DM
-WRN
-WRN
Ohms
Seed cells Day -3
DM Day 0
DM Day 4
Days of Differentiation
C
Human Colonic Epithelium
Donor 1
Donor 2
Donor 3
TEER (Ohms x cm2)
EM
DM
n = 15 wells
(Day 4 n = 3)
**** D0 vs. D1-3
Days of Differentiation
D
Caco-2
n = 21 wells
**** D1 vs. D3, D5, D9, D13-21
TEER (Ohms x cm2)
Days of Differentiation
E
Human Jejunal Epithelium (3 Donors)
EM
DM
n = 15 wells/
donor
**** D0 vs. D1-4
TEER (Ohms x cm2)
Days of Differentiation

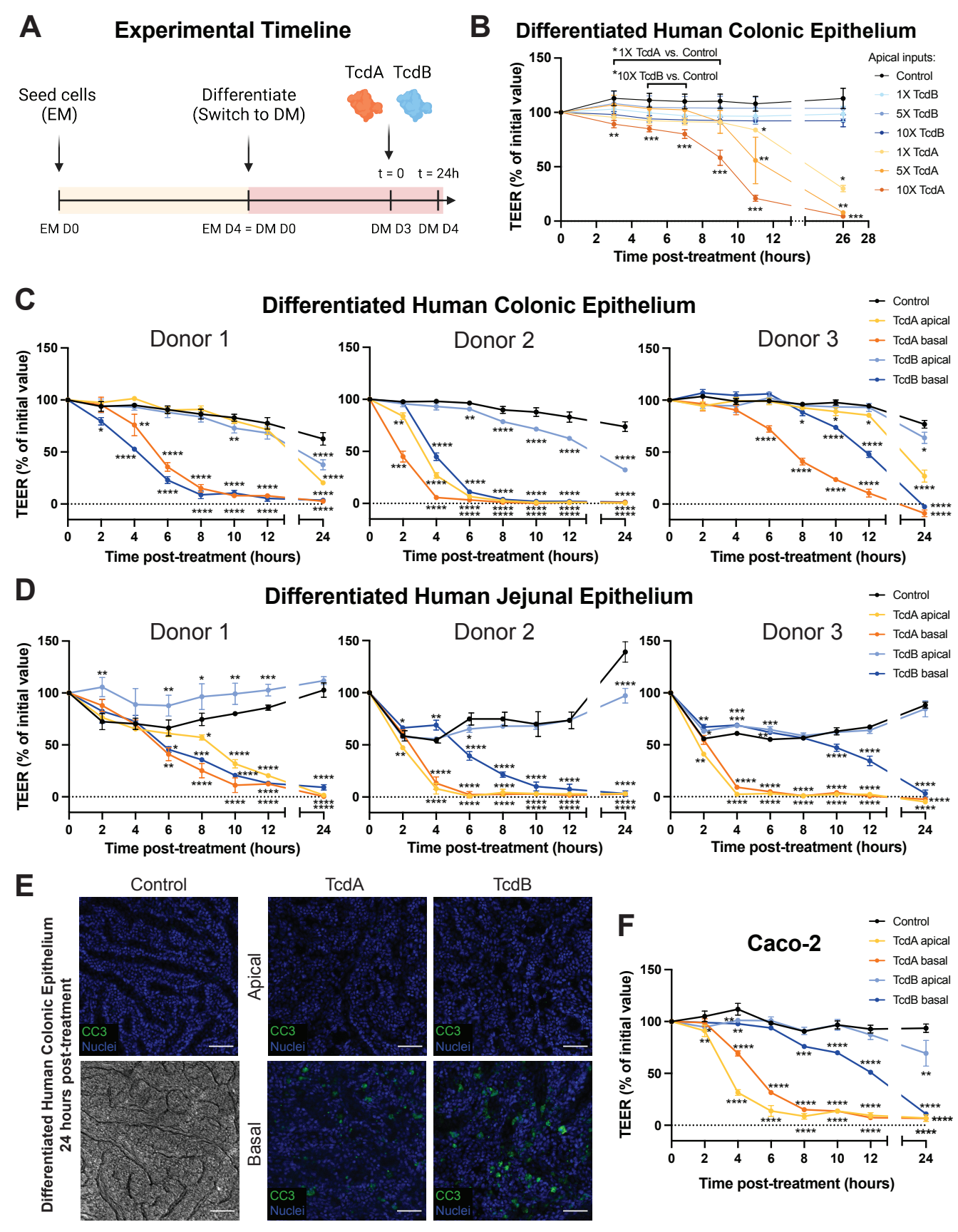
A
Experimental Timeline
Seed cells (EM)
Differentiate (Switch to DM)
TcdA TcdB
t = 0 t = 24h
EM D0
EM D4 = DM D0
DM D3 DM D4
B
Differentiated Human Colonic Epithelium
*1X TcdA vs. Control
*10X TcdB vs. Control
Apical inputs:
Control
1X TcdB
5X TcdB
10X TcdB
1X TcdA
5X TcdA
10X TcdA
TEER (% of initial value)
Time post-treatment (hours)
C
Differentiated Human Colonic Epithelium
Donor 1
Donor 2
Donor 3
Control
TcdA apical
TcdA basal
TcdB apical
TcdB basal
TEER (% of initial value)
Time post-treatment (hours)
D
Differentiated Human Jejunal Epithelium
Donor 1
Donor 2
Donor 3
Control
TcdA apical
TcdA basal
TcdB apical
TcdB basal
TEER (% of initial value)
Time post-treatment (hours)
E
Control
TcdA
TcdB
Apical
Basal
Differentiated Human Colonic Epithelium 24 hours post-treatment
CC3
Nuclei
F
Caco-2
Control
TcdA apical
TcdA basal
TcdB apical
TcdB basal
TEER (% of initial value)
Time post-treatment (hours)

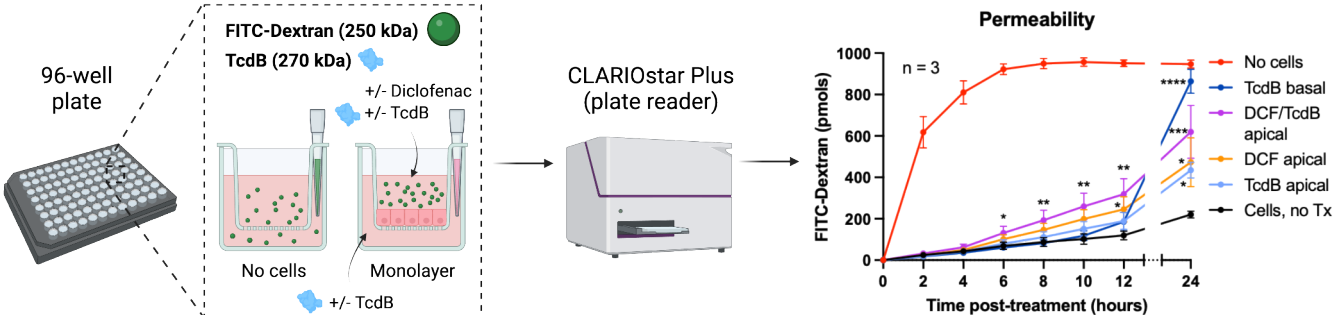
96-well plate
FITC-Dextran (250 kDa)
TcdB (270 kDa)
+/- Diclofenac
+/- TcdB
No cells
Monolayer
+/- TcdB
CLARIOstar Plus (plate reader)
Permeability
n = 3
FITC-Dextran (pmols)
Time post-treatment (hours)
No cells
TcdB basal
DCF/TcdB apical
DCF apical
TcdB apical
Cells, no Tx

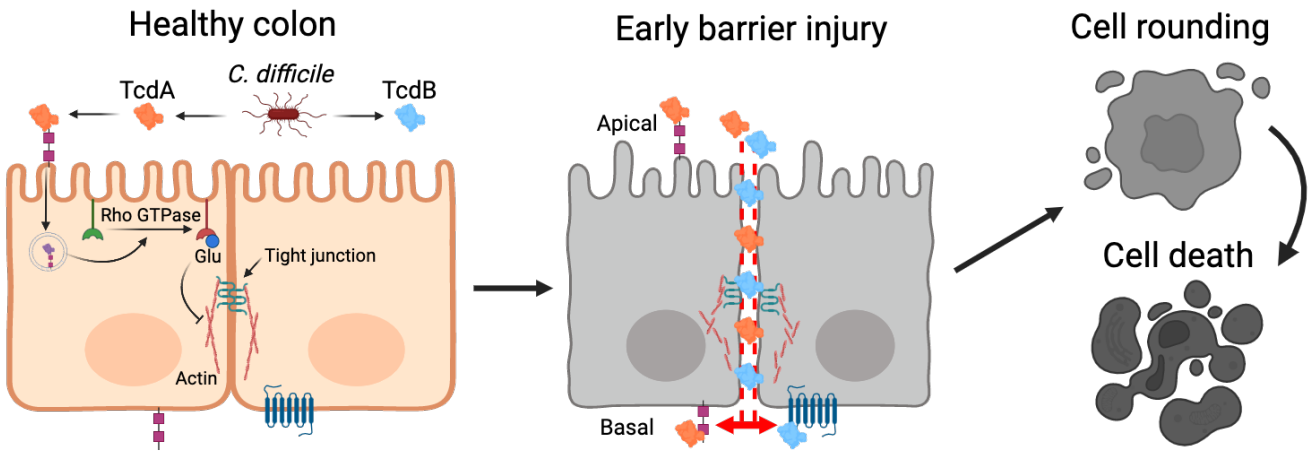
Healthy colon
C. difficile
TcdA
TcdB
Rho GTPase
Glu
Tight junction
Actin
Early barrier injury
Apical
Basal
Cell rounding
Cell death

Table 1. Formulations of primary cell culture media

Component	Stock concentration	Vendor / Catalog #	Volume required for 500 mL (final concentration)		
			EM (Small Intestine)	EM (Colon)	DM
L-WRN conditioned medium[a]	N/A	N/A	250 mL (50%, v/v)	250 mL (50%, v/v)	-
Adv. DMEM/F12	1X	ThermoFisher, 12634010	225 mL (45%, v/v)	230 mL (46%, v/v)	490 mL (98%, v/v)
GlutaMAX	100X	ThermoFisher, 35050061	2.5 mL (1X)[b]	2.5 mL (1X)[b]	5 mL (1X)
HEPES	1 M	Corning, 25-060-CI	5 mL (10 mM)	5 mL (10 mM)	5 mL (10 mM)
Primocin	50 mg/mL	Invivogen (VWR), mspp-ant-pm2	500 µL (50 µg/mL)	500 µL (50 µg/mL)	500 µL (50 µg/mL)
Pen/Strep	100X	ThermoFisher 15070063	2.5 mL (1X)[b]	2.5 mL (1X)[b]	-
N-acetylcysteine	500 mM	Sigma-Aldrich, A9165	1.25 mL (1.25 mM)	1.25 mL (1.25 mM)	1.25 mL (1.25 mM)
EGF, murine	1 mg/mL	Peprotech, 315-09	25 µL (50 ng/mL)	25 µL (50 ng/mL)	25 µL (50 ng/mL)
Nicotinamide	1 M	Sigma-Aldrich, N0636	5 mL (10 mM)	-	-
B27 Supplement	50X	ThermoFisher, 12587001	10 mL (1X)	10 mL (1X)	-
Gastrin	100 µM	Sigma-Aldrich, G9145	50 µL (10 nM)	50 µL (10 nM)	-
Prostaglandin E2	1 mM	Peprotech, 3632464	5 µL (10 nM)	-	-
A 83-01	500 µM	Sigma-Aldrich, SML0788	-	500 µL (500 nM)	500 µL (500 nM)
SB202190	30 mM	Peprotech, 1523072	50 µL (3 µM)	50 µL (3 µM)	-
Y-27632	10 mM	Selleck Chemical, S6390	500 µL (10 µM)	500 µL (10 µM)	-
Fetal Bovine Serum	N/A	VWR, 97068-085	0 mL (10%, v/v)[b]	0 mL (10%, v/v)[b]	-

[a]Prepared by culture of L-WRN cell line (ATCC, CRL-3276) and harvesting medium containing Wnt3a, R-spondin 3, and noggin.
[b]Final concentration reflects ~1:1 mixture with L-WRN conditioned media, which contains Adv. DMEM/F12 (78% v/v), Fetal Bovine Serum (20% v/v), GlutaMAX (1X), and Pen/Strep (1X). No additional FBS is added to EM.

Table 2. Formulation of Caco-2 media

Component	Stock concentration	Vendor / Catalog #	Volume required for 500 mL (final concentration)
DMEM	1X	ThermoFisher, 11995065	445 mL (89%, v/v)
Fetal Bovine Serum	N/A	VWR, 97068-085	50 mL (10%, v/v)
Pen/Strep	100X	ThermoFisher, 15070063	5 mL (1X)